Journal of Medicinal Chemistry

Article

Chemical Control of Mammalian Circadian Behavior through Dual Inhibition of Casein Kinase I# and

Jae Wook Lee, Tsuyoshi Hirota, Daisuke Ono, Sato Honma, Ken-ichi Honma, Keunwan Park, and Steve Kay

J. Med. Chem., **Just Accepted Manuscript** • DOI: 10.1021/acs.jmedchem.8b01541 • Publication Date (Web): 01 Feb 2019

Just Accepted

ACS Publications

is published by the American Chemical Society. 1155 Sixteenth Street N.W., Washington, DC 20036

Chemical Control of Mammalian Circadian Behavior through Dual Inhibition of Casein Kinase Iα and δ

Jae Wook Lee[1,5,#,*], Tsuyoshi Hirota[2,#,*], Daisuke Ono[3], Sato Honma[3], Ken-ichi Honma[3], Keunwan Park[4], Steve A. Kay[2,6]

[1]Natural Product Research Center, Korea Institute of Science and Technology, Gangneung 25451, South Korea.

[2]Institute of Transformative Bio-Molecules, Nagoya University, Nagoya, 464-8601, Japan.

[3]Department of Physiology, Graduate School of Medicine, Hokkaido University, Sapporo, 060-8638, Japan.

[4]Natural Product Informatics Research Center, Korea Institute of Science and Technology, Gangneung, 25451, South Korea.

[5]Convergence Research Center for Dementia, Korea Institute of Science and Technology, Seoul, South Korea.

[6]Keck School of Medicine, University of Southern California, Los Angeles, CA 90089, USA.

[#]JWL and TH contributed equally.

*Correspondence: Jae Wook Lee (jwlee5@kist.re.kr) and Tsuyoshi Hirota (thirota@itbm.nagoya-u.ac.jp)

Current address of D.O.: Department of Neuroscience II, Research Institute of Environmental Medicine, Nagoya University, Furo-cho, Chikusa-ku, Nagoya 464-8601, Japan

Abstract

Circadian rhythms are controlled by transcriptional feedback loops of clock genes and proteins. The stability of clock proteins is regulated by post-translational modification, such as phosphorylation by kinases. In particular, casein kinase I (CKI) phosphorylates PER protein to regulate proteasomal degradation and nuclear localization. Therefore, CKI inhibition can modulate mammalian circadian rhythms. In the present study, we have developed novel CKIα and CKIδ dual inhibitors by extensive structural modification of N9 and C2 position of longdaysin. We identified NCC007 that showed stronger period effects (0.32 μM for 5-hr period lengthening) in cell-based circadian assay. The following *in vitro* kinase assay showed that NCC007 inhibited CKIα and CKIδ with IC_{50} of 1.8 μM and 3.6 μM. We further demonstrated that NCC007 lengthened period of mouse behavioral rhythms *in vivo*. Thus, NCC007 is a valuable tool compound to control circadian rhythms through CKI inhibition.

INTRODUCTION

In mammals, circadian rhythms of behavior and physiology are controlled by molecular circadian clock. The circadian clock is constituted by transcriptional feedback loops of clock genes and their protein products. CLOCK (Circadian Locomotor Output Cycles Kaput) and BMAL1 (Brain and Muscle Aryl hydrocarbon receptor nuclear translocator-Like) transcription factors activate the transcription of other clock genes (*Per* (*Period*) and *Cry* (*Cryptochrome*)). The PER (PER1, PER2, and PER3) and CRY (CRY1

and CRY2) proteins repress their own transcription by blocking CLOCK and BMAL1 mediated transcription.[1,2]

The cellular circadian clocks are organized in a hierarchical manner. The suprachiasmatic nucleus (SCN) constitutes the central circadian pacemaker regulating behavioral rhythms.[3] On the other hand, peripheral clocks in other tissues control rhythmic outputs such as retinal visual processing[4], hepatic glucose production[5], and heart rate[6]. Disturbance of clock function has been associated with various pathologies[7] including circadian sleep disorder[8], cardiovascular disease[9], cancer[10], and metabolic disease[11].

The clock proteins are regulated by post-translational modifications such as phosphorylation for control of stability[12] and protein-protein interaction.[13] Several kinases have been reported to phosphorylate clock proteins.[14] For instance, casein kinase I (CKI) δ and ε phosphorylate PER protein to regulate proteasome-dependent degradation and nuclear localization.[15] Mutation of CKIδ or phosphorylation site of PER2 causes familial advanced sleep phase (FASP) in humans.[16,17] Considering close association of circadian clock with kinase functions, small-molecule kinase modulators may lead to new treatments for circadian disorder.[18,19]

To date, numbers of small molecules have been reported as modulators of circadian period in cultured cells including a CDK inhibitor roscovitine[20]; a p38 MAPK inhibitor SB203580[21]; a JNK inhibitor SP600125[22]; and CKIδ/ε inhibitors PF-670462[23], IC261[15], CKI-7[24], and D4476[25]. We previously identified a 2-benzylaminopurine derivative, longdaysin, as a potent modulator of circadian rhythms through high-throughput screening.[26] CKIα, CKIδ, and ERK2 mitogen-activated protein kinase were

identified as the targets of longdaysin by affinity-based proteomic analysis. Among them, CKIα and CKIδ play a major role in circadian period change. Thus, the dual inhibition of CKIα and CKIδ potently modulates the mammalian circadian rhythm.[26] In this study, we designed and synthesized the focused-library of longdaysin-derived purine scaffolds. Structure activity relationship (SAR) of the derivatives for circadian clock regulation was investigated. A series of analogues designated as "NCC compounds" were identified with potent circadian period-lengthening activities in cells. More importantly, a compound NCC007 exhibited *in vivo* efficacy to control behavioral rhythms in mice.

RESULT AND DISCUSSION

Design, synthesis and activities of longdaysin derivatives

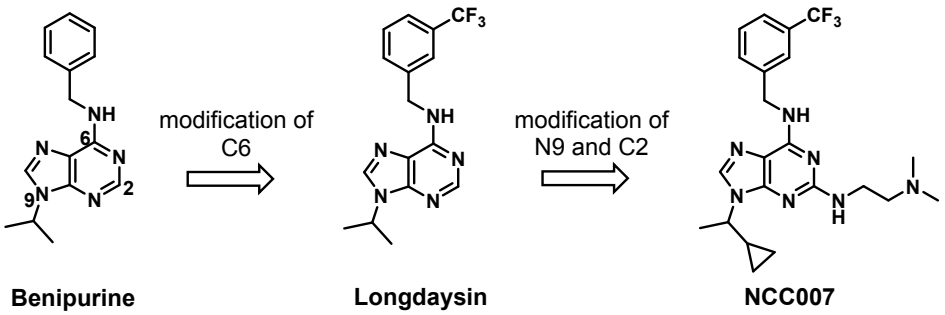

Figure 1. Design and synthesis of longdaysin derivatives.

In the initial SAR study of benipurine, a hit compound of our cell-based circadian screen, we identified longdaysin with better potency (**Figure 1**).[26] The derivatives on substituent of N9 position showed decreased activity expect isopropyl substituent. Modification of C6 revealed that 3-trifluorobenzyl group is potent structure among various substituted benzyl group. Especially, *meta*-CF_3 benzyl amine produced the most potent compound[26]. The compound longdaysin showed submicromolar activity for 1-hr period lengthening (0.3 μM), which was 3-fold more potent than benipurine (0.9 μM for 1-hr). We aimed to develop further potent compounds with better solubility for mouse behavioral study.

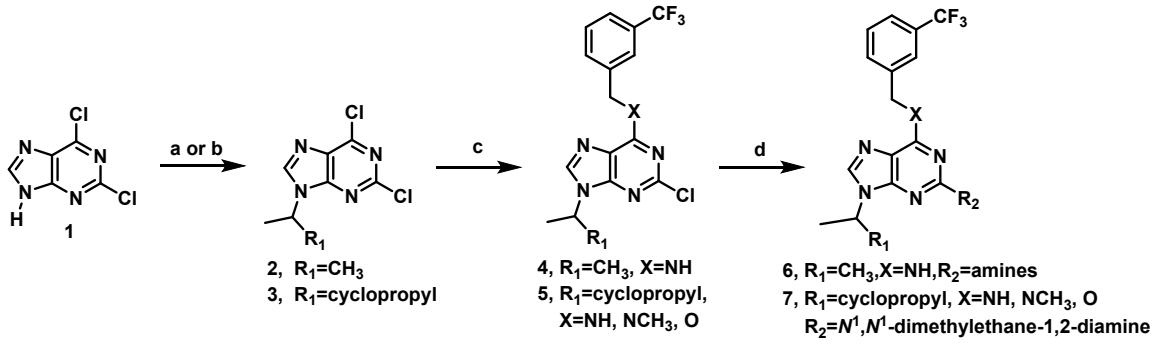

Scheme 1. (a) DEAD, Ph_3P, isopropyl alcohol, THF, 0°C (b) 1-cyclopropyl ethyl alcohol, DEAD, Ph_3P, THF, 0°C (c) 3-trifluoromethylbenzylamine, DIEA, *n*-BuOH, 60°C; or 3-trifluoromethylbenzyl methylamine, DIEA, n-BuOH, 60°C; or 3-trifluoromethylbenzyl alcohol, NaH, DMF, 80°C (d) R_2NH_2, DIEA, *n*-BuOH, 120°C; or R_2OH, NaH, DMF, 120°C

In the present study, we conducted optimization of longdaysin by focusing on unexplored C2 position. As shown in **Scheme 1**, Mitsunobu reaction of commercially available purine **1** with isopropyl alcohol or 2-ethylcyclopropyl alcohol provided intermediate **2** or **3**, which were further transformed into the desired analog **4** and **5** via a sequence of 3-trifluorobenzylamine substitution. Analogues **6** and **7** were prepared in relatively high yield by similar procedure using various aryl or alkyl amines.

Table 1. Cellular activity of longdaysin derivatives.

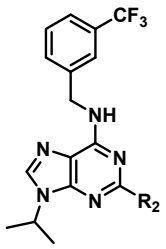

Compound	R_2	Circadian period lengthening	
		1-hr (μM) [a]	5-hr (μM) [a]
longdaysin	H	0.39	3.4
6a	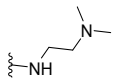	0.09	0.9
6b	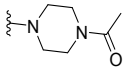	1.03	5.7
6c	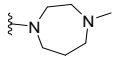	0.68	5.8
6d	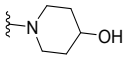	1.98	10.43
6e	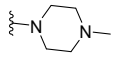	0.90	3.66
6f	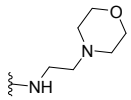	1.65	9.33
6g		1.62	3.04
6h	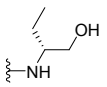	0.38	3.76
6i	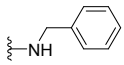	Inactive	Inactive
6j	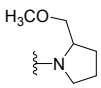	Inactive	Inactive

6k	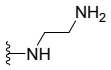	0.58	5.23
6l		0.32	2.39
6m		0.39	2.75
6n	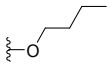	6.39	23.36

[a] value is the compound concentration required to produce 1-hr and 5-hr circadian period lengthening effects. Each value is the mean of at least two independent determinations,

We examined the effect of various functional groups with alkyl and benzyl substitution on C2 position of purine scaffold in cell-based circadian assay (**Table 1**). Alkyl and benzyl substitution derivatives was less potent than or similar to longdaysin. In contrast, 0.9 μM of 6a caused 5-hr period lengthening, which was ~3-fold more potent than longdaysin. In parallel, we designed and synthesized longdaysin derivative 7a with N9 1-cyclopropyl ethyl group. 7a showed ~3-fold more potent effect than longdaysin (**Table 2**). Based on this SAR information, we designed to combine N9 substitution of 7a and C2 substitution of 6a and synthesized "7b (NCC007)" which showed ~10-fold more potency than longdaysin (**Figure 2**). To investigate the role of C6 nitrogen, we designed and synthesized the N-methyl analogue 7c and O-analogue 7d to eliminate potential hydrogen bond interaction (**Table 2**). As expected, they showed dramatic decrease in period lengthening activity. Therefore, they can be used as negative controls. On the basis of structure activity relationship and extended synthesis, we discovered 7b (NCC007) as the most potent compound.

Table 2. Cellular activity of NCC007 derivatives.

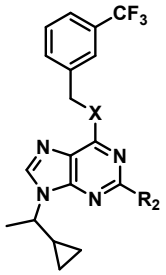

Compound	X	R_2	Circadian period lengthening	
			1-hr (μM) [a]	5-hr (μM) [a]
7a	NH	H	0.09	0.9
7b (NCC007)	NH	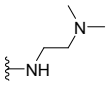	0.022	0.32
7c	CH_3N	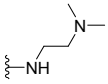	Inactive	Inactive
7d	O	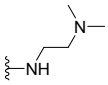	Inactive	Inactive

[a] value is the compound concentration required to produce 1-hr and 5-hr circadian period lengthening effects. Each value is the mean of at least two independent determinations,

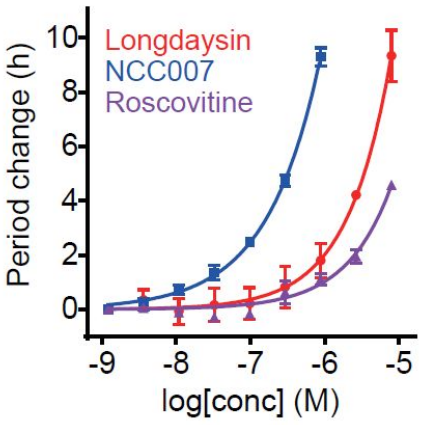

	1 hr (μM)	5 hr (μM)
Longdaysin	0.39	3.4
NCC007	0.022	0.32
Roscovitine	0.96	9.0

Figure 2. Effects of NCC007, longdaysin and roscovitine on the period length of cellular circadian rhythms.

Inhibitory effect of NCC007 toward CKIα correlates with period phenotype.

We previously revealed that longdaysin inhibits CKIα and CKIδ.[26] We analyzed the effects of 5 μM NCC007 and longdaysin against 57 kinases from a variety of classes (**Figure 3A**). Longdaysin inhibited CKIδ, CKIα, CDK2, CDK7, and MAPK1 by >30%. The effects on CKIδ, CKIα, and CDK7 were enhanced in NCC007, while the effects on CDK2 and MAPK1 were reduced. We then analyzed IC_{50} values of longdaysin, NCC007, and roscovitine against these kinases (**Figure 3B**). CKIα was the most potently inhibited kinase of NCC007 and the only kinase correlated with circadian period lengthening activities (**Figure 2**) in which the activity order was NCC007>longdaysin>roscovitine. We further conducted profiling of total 374 kinases (including 57 kinases in **Figure 3A**) by using 5 μM NCC007 (**Figure 3C** and **Table S2**). Again, CKIα (CK1a1) was the most inhibited kinase supporting an important role of CKIα in the regulation of circadian period by NCC007. Only 9 kinases among 374 kinases were inhibited by more than 50%. In addition to CKI family (CKIα, CKIδ, CKIα-like, and CKIε) and CDK family (CDK7 and CDK6) proteins, SRPK2, SRPK1, and CLK2 were found to be inhibited by NCC007 with much less effect than CKIα. SRPK2, SRPK1, and CLK2 phosphorylate SR proteins to regulate mRNA splicing, and their role in circadian regulation will be investigated in future studies. Together, NCC007 showed more selectivity against CKIα, suggesting that CKIα plays an important role in regulation of circadian period.

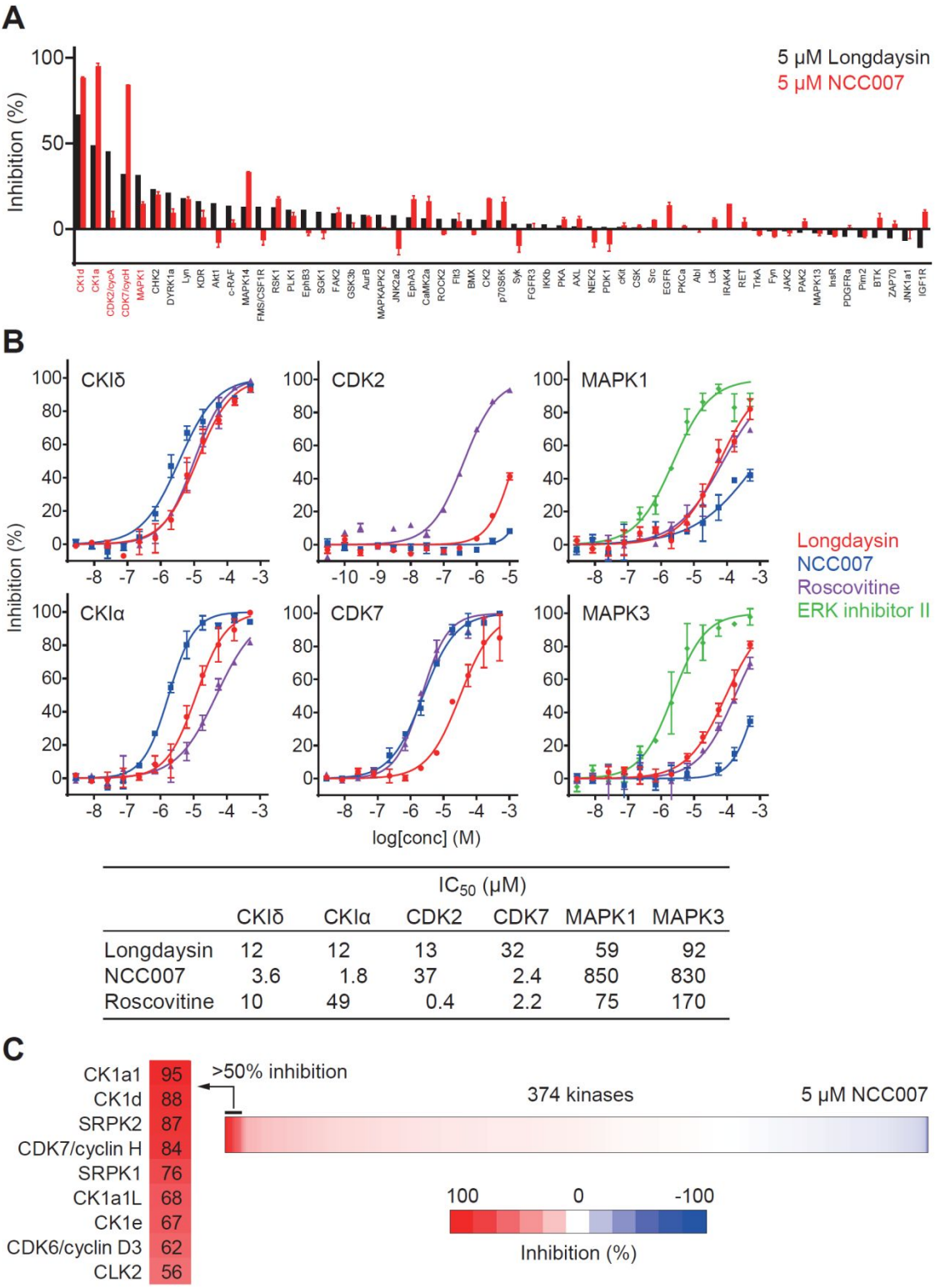

	IC_{50} (μM)					
	CKIδ	CKIα	CDK2	CDK7	MAPK1	MAPK3
Longdaysin	12	12	13	32	59	92
NCC007	3.6	1.8	37	2.4	850	830
Roscovitine	10	49	0.4	2.2	75	170

Figure 3. Effects of NCC007 and longdaysin on kinase activities. (A) Profiling of NCC007 and longdaysin toward 57 kinases. (B) *In vitro* assay of CKIδ, CKIα, CDK2, CDK7, MAPK1, and MAPK3 to Longdaysin,

NCC007, and Roscovitine. (C) Profiling of NCC007 toward 374 kinases. Kinases inhibited by >50% were highlighted in left.

Molecular modeling studies suggests NCC007 has stronger binding affinity toward CKIα and CKIδ than longdaysin.

Based on the results of the kinase assay, we performed molecular docking simulations to present plausible binding models of longdaysin and NCC007 for human CK1α. NCC007 is a racemic mixture that has R and S enantiomers. Because of difficulties in evaluating each enantiomer experimentally, we investigated them computationally. RosettaLigand docking protocol was written by using RosettaScript and used to optimize docking conformations. The lowest binding energy conformation from 5,000 docking experiments was considered as the final docking model shown in **Figure 4**.

Rosetta energy scores for the final docking models were −25.28, −25.71, and −22.22 (Rosetta Energy Unit) for R-NCC007, S-NCC007, and longdaysin, respectively. Binding energy of R- and S-forms of NCC007 was almost comparable and lower than longdaysin, consistent with the stronger inhibition of CK1α by NCC007 than longdaysin. In the docking model, longdaysin fit into the hydrophobic pocket formed by Ile31, Ala44, Leu93, Pro95, Leu143, and Ile156, and especially, the benzyl amino group of londaysin formed hydrogen bonds with the backbone of Leu93 (**Figure 4A**).

R- and S-NCC007 fit to the longdaysin-binding pocket, and showed more extensive contacts to CK1α (**Figures 4B** and **4C**). R-NCC007 fit very well into the hydrophobic binding pocket consisted of Ile23, Ile31, Ala44, Met90, Leu93, and Leu143. Moreover, the fluorine group in NCC007 showed additional polar interactions with Lys46, Tyr64,

and Asp157 in the varied binding pocket (**Figure 4B**) with high shape complementarity. On the other hand, docking model of S-NCC007 showed the lowest binding energy (−25.71) mainly by the hydrophobic interactions, which is more similar to the docking model of longdaysin that the fluorine group is exposed to the solvent (**Figure 4C**). Taken together, the docking models suggest that NCC007 likely binds to CK1α with more favorable interactions and higher shape complementarity than longdaysin regardless of R and S configurations.

In the docking model, the C2 position of longdaysin is located near the solvent-accessible void space in the binding pocket (**Figure 4A**), thus **6a** with adequate volume fitting to the void space might show enhanced activity. In contrast, the derivatives of bulky functional group such as **6d** and **6f** had decreased activity by clashing to the binding pocket. Despite the chemical similarity, **6k** showed much less activity compared to **6a**, probably due to more favorable contacts through the methyl groups in **6a**. Alternatively, primary amine of **6k** may easily bind to cellular metabolites such as bioaldehyde, resulting in less cellular activity compared with **6a**.

Similar to CK1α, we observed lower binding energy of R-NCC007 (-26.97) and S-NCC007 (-25.55) than longdaysin (-21.73) against CK1δ (**Figure S1**), consistent with kinase assay result. However, due to high structural similarity (Cα RMSD 0.487) and identical binding residues between CKIα and CKIδ (**Figures S2 and S3**), it is difficult to explain the 2-fold activity difference of NCC007 against CKIα and CKIδ.

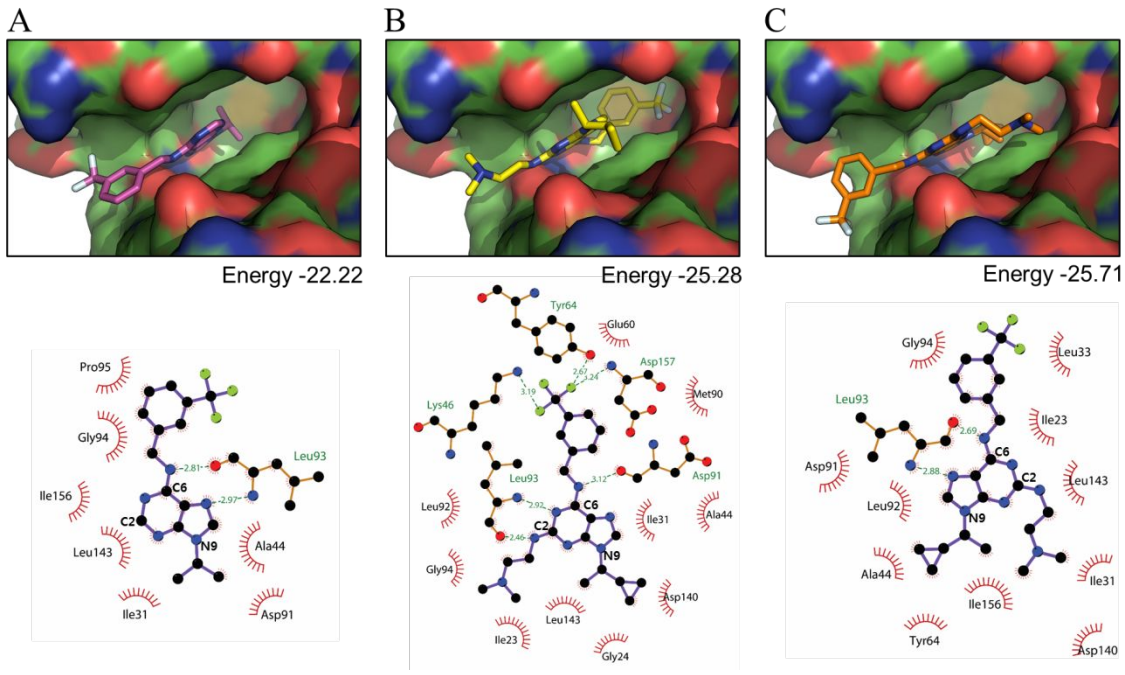

Figure 4. Comparison of binding modes of (A) longdaysin (carbon atoms in magenta), (B) NCC007 R-form (carbon atoms in yellow), and (C) NCC007 S-form (carbon atoms in orange) are presented by RosettaLigand docking experiment. To clarify the binding modes, the protein is represented by surface and the docked ligands are shown by sticks. All protein figures are created with PyMOL software[27]. Two-dimensional interaction maps are shown together for the residues in the binding pocket by LIGPLOT software[28]. Hydrogen bonds are depicted with a dotted line.

Lengthening of behavioral circadian rhythms *in vivo* by longdaysin and NCC007.

To extend these findings to the *in vivo* application, pharmacological inhibition of both CKIα and CKIδ by longdaysin and NCC007 were tested in mice. Compounds were infused into the lateral ventricle using osmotic pump. This approach has advantage to avoid possible blood brain barrier penetration problem. Mice were entrained to 12-hr light and 12-hr dark cycles, then released to constant darkness where they show ~23.8-hr rhythms based on endogenous circadian clock (**Figure 5**). After artificial cerebrospinal fluid infusion as a control, 1 mM or 3 mM of longdaysin was continuously infused.

Period of circadian behavior recorded by infrared sensor[29] was lengthened about 0.05 hr by 1 mM longdaysin infusion and 0.1 hr by 3 mM longdaysin infusion. We then increased concentration of longdaysin to 5 mM or 15 mM, and 0.1 hr or 0.15 hr period lengthening was observed, respectively. Following administration of NCC007 showed more period lengthening effect with 0.15 hr at 5 mM and 15 mM. The period length returned normal by buffer infusion after NCC007 treatment, demonstrating that the effect is reversible. This result indicated that the compounds are able to control circadian behavior *in vivo*.

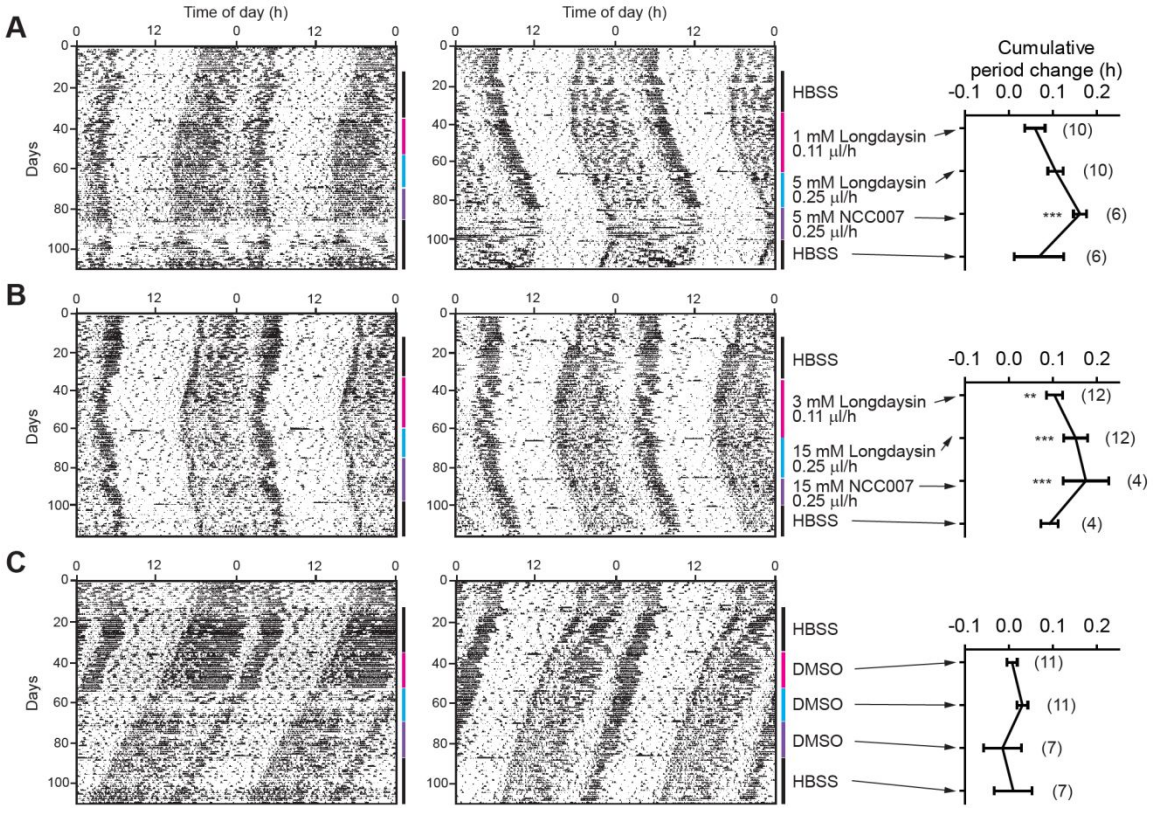

Figure 5. Circadian behavior of longdaysin and NCC007-treated mice. Mice were treated with compounds and their circadian behavior was recorded by infrared sensor under constant dark condition. (A) HBSS, 1 mM longdaysin, 5 mM longdaysin, and 5 mM NCC007 were sequentially infused into mouse brain. (B)

HBSS, 3 mM longdaysin, 15 mM longdaysin, and 15 mM NCC007 were sequentially infused. (C) DMSO infusion as negative control. The number in parenthesis indicates the number of mice. ***$p < 0.001$, **$p < 0.01$ against the DMSO control by two-way ANOVA, followed by a Tukey's multiple comparisons test.

While longdaysin and NCC007 caused more than hours of period lengthening in cell based assay, they showed much less period effect *in vivo*, although they were infused inside of the blood-brain barrier. It is likely that enough amounts of longdaysin and NCC007 may not be exposed into mouse brain, possibly due to low exposure and/or early clearance of compounds. The alternate possibility could be that CKI inhibition has less effect on circadian period *in vivo*. Consistently, Meng and coworkers reported that a potent CKIδ inhibitor, PF-670462, also caused only small period change *in vivo*.[30]

CONCLUSION

The CKI family of serine and threonine kinases is highly conserved and ubiquitously expressed in eukaryotes. Among this family, CKIδ, CKIε, and CKIα are known to play important roles in modulating circadian rhythms by phosphorylation of PER protein and stimulation of its degradation. We discovered and optimized longdaysin analogues as novel class of CKIα and CKIδ dual inhibitors that affect circadian period length. The ethyl cyclopropyl-containing analogues showed improved period lengthening effect over their isopropyl counterparts, of which the 3-trifluoro and benzylamine-containing NCC007 (**7b**) exhibited optimal period lengthening effect. We further demonstrated that NCC007 inhibited CKIα and CKIδ in *in vitro* kinase assay and showed period lengthening effect on mouse models. We believe that NCC007 proves a useful tool for studies of circadian rhythms and may ultimately lead to chronotherapeutic agents.

EXPERIMENTAL SECTION

General Procedure. All chemicals and solvents, commercially available, were purchased from commercial suppliers (Acros, Alfa Aesar and Aldrich) and used without further purification. All chemical reactions were performed under nitrogen atmosphere. Anhydrous solvents were obtained by passage through an activated alumina column. Analytical thin-layer chromatography (TLC) was performed on pre-coated glass TLC plates (layer 0.2 mm silica gel 60 with fluorescent indicator (UV 245: Merck). The TLC plates was revealed by exposure of UV lamp (254/350 nm). Column chromatography was performed using silica gel 60 (70-230 mesh; Merck). Liquid chromatography-mass

spectrometry (LC-MS) were analyzed with LC-MS (Agilent Technology 1200), using a C_{18} column, with 20 minutes elution using a gradient solution of CH_3CN-H_2O (containing 0.05% trifluoroacetic acid), with UV detector and an electrospray ionization source. The purity of all compounds were analyzed by the analytical LC-MS system describe, and purity >95%. The molecular mass was evaluated using the analytical LC-MS system. ^1H and ^{13}C NMR spectral data were obtained from a Bruker Avance II 400 MHz spectrometer. Chemical shifts (δ) are reported relative to internal $CDCl_3$ (Me_4Si, δ 0.0) and CD_3OD (Me_4Si, δ 0.0). Signal splitting patterns are described as singlet (s), doublet (d), triplet (t), multiplet (m), or a combination thereof. Coupling constants (J) are quoted to the nearest 0.1 Hz.

The synthesis of 2,6-dichloro-9-isopropylpurine (2). Anhydrous tetrahydrofuran (100.0 ml) is added to a flame-dried flask under N_2 containing 2-chloro-6-chloropurine (2.00 g, 0.01 mol) and triphenylphosphine (5.24 g, 0.02 mol). To this 2-propanol (1.87 mL, 0.025 mol) is added, and the mixture is then cooled to -10°C by using an ethylene glycol/dry-ice bath. After dropwise addition of diethyl azodicarboxylate (3.14 mL, 0.02 mol), the mixture is warmed gradually to room temperature. After 12 h, the reaction is quenched with 1 mL of water and the solvent is removed in vacuo. The resulting yellow oil is purified by column chromatography (1.0 L of SiO_2, eluted with 100% CH_2Cl_2). The resulting solid is triturated with methanol to yield 1.53 g (66.5%) of a compound 2 as a white solid**.** ^1H NMR (400 MHz, $CDCl_3$) δ 8.20 (s, 1H), 4.91 (dd, J = 13.5 Hz, 6.8 Hz, 1H), 1.66 (d, J = 6.8 Hz, 6H). ^{13}C NMR (100 MHz, $CDCl_3$) δ 152.7, 151.7, 143.6, 132.9, 131.0, 48.2, 22.5. ESI-MS: m/z calcd for $C_8H_9Cl_2N_4$ [M+H] = 231.0 found 231.1.

The synthesis of 2,6-dichloro-9-(1-cyclopropylethyl)purine (3). The solution of compound **1** (1.00 g, 5.32 mmol) and triphenylphosphine (2.79 g, 10.64 mmol) in anhydrous tetrahydrofuran (50 mL) was cooling down at -10°C by using an ethylene glycol/dry ice bath. 1-cyclopropylethyl alcohol (915.8 mg, 10.64 mmol) was slowly added to the reaction. Diethyl azadicarboxylate (1.67 mL, 10.64 mmol) was slowly added over a period of 20 min under nitrogen atmosphere. The reaction mixture was stirred for 48 hr at room temperature. The reaction is quenched with 0.5 mL of water and the solvent is removed in vacuo. The residue was charged directly on silicagel column and purified with dichloromethane to yield 742 mg (54.6%) of a compound 3 as white solid. ^{1}H NMR (400 MHz, $CDCl_3$) δ 8.51 (s, 1H), 3.94-3.89 (m, 1H), 1.61 (d, J = 6.8 Hz, 3H), 1.36-1.30 (m, 1H), 0.77-0.71 (m, 1H), 0.56-0.50 (m, 1H), 0.49-0.41 (m, 1H), 0.37-0.29 (m, 1H). ^{13}C NMR (100 MHz, $CDCl_3$) δ 152.6, 151.6, 148.0, 144.1, 132.9, 57.6, 22.5, 16.8, 5.0, 4.4. ESI-MS: m/z calcd for $C_{10}H_{11}Cl_2N_4$ [M+H] = 257.0 found 257.1.

The synthesis of 2-chloro-9-isopropyl-N-(3-(trifluoromethyl)benzyl)-9H-purin-6-amine (4). The solution of compound **2** (1.53 g, 6.65 mmol) in n-BuOH (40 mL) was treated with m-trifluorobenzyl amine (1.28 g, 7.32 mmol) and DIEA (1.72 mL, 9.98 mmol). The reaction mixture was heated at 60 °C for 24 hr. After reaction was quenched with 1 mL of water, solvent was evaporated in vacuo. The reaction mixture was extracted with dichloromethane (100 mL, 3 times) and H_2O (40 mL, 3 times). Organic layer was dried with Na_2SO_4 and evaporated in vacuo. The residue was purified by silica gel column chromatography (dichloromethane : methanol = 40:1) to yield 2.12 g (86.53%) of

a compound **4** as white solid. ^{1}H NMR (400 MHz, $CDCl_3$) δ 7.94 (s, 1H), 7.68 (s, 1H), 7.65-7.54 (m, 2H), 7.49 (d, J = 8.0 Hz, 1H), 5.00-4.84 (m, 3H), 1.61 (d, J = 6.8 Hz, 6H). ^{13} C NMR (100 MHz, $CDCl_3$) δ 138.9, 137.2, 133.1, 131.4, 131.2, 130.9, 130.6, 129.2, 125.3, 124.8, 124.6, 124.5, 122.6, 47.6, 22.7. ESI-MS: m/z calcd for $C_{16}H_{16}ClF_3N_5$ [M+H] = 370.1 found 370.2.

The synthesis of 2-chloro-9-(1-cyclopropylethyl)-N-(3-(trifluoromethyl)benzyl)-9H-purin-6-amine (5). The solution of compound **3** (500 mg, 1.95 mmol) in n-BuOH (20 mL) was treated with *m*-trifluorobenzyl amine (377 mg, 2.15 mmol) and DIEA (403 □L, 2.34 mmol). The reaction mixture was heated at 60 ^{o}C for 24 hr. After reaction was quenched with 500 μL of water, solvent was evaporated in vacuo. The residue was extracted with dichloromethane (100 mL) and H_2O (20mL). Organic layer was dried with Na_2SO_4 and evaporated in vacuo. The residue was purified by silica gel column chromatography (dichloromethane : methanol = 40:1) to yield 514.1 mg (66.73%) of a compound **5a** as white solid. ^{1}H NMR (400 MHz, $CDCl_3$) δ 7.79 (s, 1H), 7.58 (s, 1H), 7.56-7.44 (m, 2H), 7.39 (t, J = 7.6 Hz, 1H), 4.84 (s, 2H), 3.90-3.79 (m, 1H), 1.53 (d, J = 6.8 Hz, 3H), 1.40-1.25 (m, 1H), 0.71-0.62 (m, 1H), 0.52-0.42 (m, 1H), 0.41-0.32 (m, 1H), 0.31-0.22 (m, 1H). ^{13}C NMR ($CDCl_3$) δ 154.9, 154.4, 139.1, 138.2, 131.2, 130.8, 129.2, 125.3, 124.7, 124.4, 122.6, 118.2, 56.4, 44.2, 20.9, 16.9, 4.8, 4.2. ESI-MS: m/z calcd for $C_{18}H_{18}ClF_3N_5$ [M+H] = 396.1 found 396.2.

The general synthetic procedure of compounds (6). For amine substitution reaction at C6; The solution of a compound **4** (50 mg, 0.14 mmol) in n-BuOH (2mL) was treated with DIEA (48.3 μL, 0.28 mmol) and various amines (0.28 mmol, 2.0 eq.). The reaction

mixture was heated at 120 °C for 48 hr. After quenching the reaction with 100 □L of water, solvent was evaporated in vacuo. The residue was purified by prep-HPLC with H_2O-acetonitrile to yield compounds.

For alcohol substitution reaction at C6; various alcohols (0.48 mmol, 2.0 eq.) in DMF (1 mL) was treated with NaH 60% (20 mg, 0.48 mmol). The reaction mixture was stirred for 30 min at 50 °C. The solution of compound 4 (50 mg, 0.14 mmol) in DMF (1 mL) was slowly added to the reaction mixture. The reaction mixture was heated at 120 °C for 48 hr. After quenching the reaction with 100 μL of water, solvent was evaporated in vacuo. The residue was purified by prep-HPLC with H_2O-acetonitrile to yield compounds.

N2-(2-(dimethylamino)ethyl)-9-isopropyl-N6-(3-(trifluoromethyl)benzyl)-9H-purine-2,6-diamine (6a). The synthesis of 6a was followed by general procedure to yield 42.1 mg (71.4%) of a compound 6a. ^{1}H NMR (400 MHz, $CDCl_3$) δ 8.00-7.92 (m, 1H), 7.73-7.66 (m, 1H), 7.65-7.54 (m, 1H), 7.53-7.47 (m, 1H), 7.44 (t, J = 8.0 Hz, 1H), 5.29 (s, 1H), 4.78 (s, 1H), 4.69 (s, 1H), 3.83-3.75 (m, 2H), 3.32-3.25 (m, 1H), 3.20-3.05 (m, 1H), 2.86 (s, 3H), 2.76 (s, 3H), 1.53 (s, 3H), 1.52 (s, 3H). ^{13}C NMR (100 MHz, $CDCl_3$) δ 163.0, 162.6, 130.9, 129.2, 125.3, 124.6, 124.1, 122.6, 56.4, 55.7, 53.8, 48.0, 47.2, 46.7, 43.1, 40.5, 36.8, 22.2. ESI-MS: m/z calcd for $C_{20}H_{27}F_3N_7$ [M+H] = 422.2 found 422.3.

1-(4-(9-isopropyl-6-((3-(trifluoromethyl)benzyl)amino)-9H-purin-2-yl)piperazin-1-yl)ethan-1-one (6b). The synthesis of 6b was followed by general procedure to yield 39.92 mg (61.8%) of a compound 6b. ^{1}H NMR (400 MHz, $CDCl_3$) δ 7.66 (s, 1H), 7.60-

7.55 (m, 2H), 7.52 (d, J = 7.6 Hz, 1H), 7.44 (t, J = 7.6 Hz, 1H), 6.45 (s, 1H), 4.84 (s, 2H), 4.73-4.65 (m, 1H), 3.83-3.75 (m, 4H), 3.69-3.64 (m, 2H), 3.51-3.46 (m, 2H), 2.15 (s, 3H), 1.58 (s, 3H), 1.56 (s, 3H). ^{13}C NMR (100 MHz, $CDCl_3$) δ 169.2, 158.6, 154.1, 140.6, 135.1, 130.8, 130.7, 129.0, 124.4, 124.3, 124.0, 123.9, 115.5, 46.6, 46.1, 44.7, 44.3, 41.3, 22.5, 21.5. ESI-MS: m/z calcd for $C_{20}H_{27}F_3N_7O$ [M+H] = 462.2 found 462.3.

9-isopropyl-2-(4-methyl-1,4-diazepan-1-yl)-N-(3-(trifluoromethyl)benzyl)-9H-purin-6-amine (6c). The synthesis of 6c was followed by general procedure to yield 38.14 mg (60.9%) of a compound 6c. ^{1}H NMR (400 MHz, $CDCl_3$) δ 9.04 (brs, 1H), 8.14 (brs, 1H), 7.64-7.55 (m, 2H), 7.55-7.44 (m, 2H), 4.83-4.72 (m, 3H), 4.45 (brs, 1H), 4.23 (brs, 1H), 3.68 (brs, 1H), 3.46 (brs, 2H), 2.75 (brs, 4H), 2.65 (s, 3H), 2.49 (brs, 1H), 2.17 (brs, 1H), 1.63 (s, 3H), 1.62 (s, 3H). ^{13}C NMR (100 MHz, $CDCl_3$) δ 163.4, 159.2, 152.3, 140.2, 132.4, 130.8, 129.1, 125.5, 123.8, 122.8, 57.0, 55.7, 48.4, 44.7, 44.4, 44.2, 42.1, 41.0, 23.8, 22.1. ESI-MS: m/z calcd for $C_{22}H_{29}F_3N_7$ [M+H] = 448.3 found 448.3.

1-(9-isopropyl-6-((3-(trifluoromethyl)benzyl)amino)-9H-purin-2-yl)piperidin-4-ol (6d). The synthesis of 6d was followed by general procedure to yield 53.14 mg (87.4%) of a compound 6d. ^{1}H NMR (400 MHz, $CDCl_3$) δ 8.39 (brs, 1H), 7.63 (s, 1H), 7.55 (d, J = 7.20 Hz, 1H), 7.45 (d, J = 7.6 Hz, 1H), 7.39 (t, J = 7.6 Hz, 1H), 4.82-4.75(m, 1H), 4.73 (s, 2H), 4.33-4.23 (m, 2H), 3.90-3.80 (m, 1H), 3.65-3.40 (m, 1H), 3.28-3.12 (m, 2H), 1.89-1.78 (m, 2H), 1.57 (s, 3H), 1.56 (s, 3H), 1.40 (brs, 2H). ^{13}C NMR (100 MHz, $CDCl_3$) δ 159.8, 152.0, 150.0, 140.5, 132.5, 131.0, 130.8, 130.5, 128.9, 125.4, 124.5, 124.4, 123.8,

122.7, 122.8, 43.9, 41.9, 40.3, 33.7, 21.9, 10.9. ESI-MS: m/z calcd for $C_{21}H_{26}F_3N_6O$ [M+H] = 435.2 found 435.2.

9-isopropyl-2-(4-methylpiperazin-1-yl)-N-(3-(trifluoromethyl)benzyl)-9H-purin-6-amine (6e). The synthesis of 6e was followed by general procedure to yield 47.68 mg (78.6%) of a compound 6e. ^{1}H NMR (400 MHz, $CDCl_3$) δ 8.27 (s, 1H), 7.57 (s, 1H), 7.52 (d, J = 7.6 Hz, 1H), 7.46 (d, J = 7.2 Hz, 1H), 7.41 (t, J = 7.6 Hz, 1H), 4.75-4.60 (m, 5H), 3.80-3.65 (m, 2H), 3.58-3.30 (m, 4H), 2.78 (s, 3H), 1.55 (d, J = 6.8 Hz, 6H). ^{13}C NMR (100 MHz, $CDCl_3$): δ 158.4, 152.7, 150.0, 140.0, 134.3, 130.8, 130.7, 130.4, 129.0, 125.4, 124.1, 124.0, 123.9, 123.8, 122.7, 53.1, 43.3, 41.5, 22.0. ESI-MS: m/z calcd for $C_{21}H_{27}F_3N_7$ [M+H] = 434.2 found 434.3.

9-isopropyl-N2-(2-morpholinoethyl)-N6-(3-(trifluoromethyl)benzyl)-9H-purine-2,6-diamine (6f). The synthesis of 6f was followed by general procedure to yield 28.71 mg (44.3%) of a compound 6f. ^{1}H NMR (400 MHz, $CDCl_3$) δ 7.85 (s, 1H), 7.74-7.66 (m, 1H), 7.65-7.59 (m, 1H), 7.56 (d, J = 7.6 Hz, 1H), 7.49 (dd, J = 8.0 Hz, 7.6 Hz, 1H), 5.34 (s, 1H), 4.85 (s, 1H), 4.76 (s, 1H), 4.00-3.92 (m, 4H), 3.90-3.79 (m, 2H), 3.20-2.96 (m, 6H), 1.57 (d, J = 6.8 Hz, 6H). ESI-MS: m/z calcd for $C_{22}H_{29}F_3N_7O$ [M+H] = 464.2 found 464.3.

9-isopropyl-N2-(cyclopropyl)-N6-(3-(trifluoromethyl)benzyl)-9H-purine-2,6-diamine (6g). The synthesis of 6g was followed by general procedure to yield 19.20 mg (35.2%) of a compound 6g. ^{1}H NMR (400 MHz, $CDCl_3$) δ 7.74-7.71 (m, 1H), 7.66-7.61 (m, 1H),

7.58-7.54 (m, 1H), 7.51-7.46 (m, 1H), 5.91 (brs, 1H, -NH), 5.35-5.33 (m. 1H), 4.90-4.80 (m, 1H), 4.73-4.65 (m, 1H), 1.59 (d, J = 6.8 Hz, 3H, -CH_3), 1.56 (d, J = 6.8 Hz, 3H, -CH_3), 1.01-0.99 (m, 1H), 0.90-0.80 (m, 2H), 0.70-0.60 ppm (m, 2H). ^{13}C NMR (100 MHz, $CDCl_3$) δ 163.1, 162.7, 149.4, 138.2, 137.8, 132.1, 131.0, 129.3, 125.3, 117.8, 114.8, 58.1, 42.7, 29.7, 22.4, 22.2, 7.1, 7.0. ESI-MS: m/z calcd for $C_{19}H_{22}F_3N_6$ [M+H] = 391.2 found 391.2.

(R)-2-((9-isopropyl-6-((3-(trifluoromethyl)benzyl)amino)-9H-purin-2-yl)amino)butan-1-ol (6h). The synthesis of 6h was followed by general procedure to yield 23.9 mg (40.4%) of a compound 6h. ^{1}H NMR (400 MHz, $CDCl_3$) δ 9.11 (s, 1H), 8.26 (s, 1H), 7.75 (s, 1H), 7.68 (d, J = 7.2 Hz, 1H), 7.62 (d, J = 7.6 Hz, 1H), 7.57 (t, J = 7.6 Hz, 1H), 4.78 (brs, 1H), 4.73 (brs, 1H), 4.61 (dd, J = 13.2 Hz, 6.8Hz, 1H), 3.84 (s, 1H), 3.52-3.45 (m, 1H), 1.70-1.60 (m. 1H), 1.51 (d, J = 3.6 Hz, 3H), 1.49 (d, J = 3.2 Hz, 3H), 1.48 (s, 3H), 0.88-0.82 (m, 2H). ^{13}C NMR (100 MHz, $CDCl_3$) δ 159.1, 131.5, 129.4, 129.2, 128.9, 125.5, 124.0, 123.9, 123.7, 122.8, 62.2, 54.5, 47.2, 43.0, 23.6, 21.8, 21.7, 10.3. ESI-MS: m/z calcd for $C_{20}H_{26}F_3N_6O$ [M+H] = 423.2 found 423.3.

N2-benzyl-9-isopropyl-N6-(3-(trifluoromethyl)benzyl)-9H-purine-2,6-diamine (6i). The synthesis of 6i was followed by general procedure to yield 34.5 mg (56.9%) of a compound 6i. ^{1}H NMR (400 MHz, $CDCl_3$) δ 8.47 (brs, 1H), 8.17 (s, 1H), 7.71 (s, 1H), 7.60 (d, J = 7.6 Hz, 2H), 7.55-7.47 (m, 1H), 7.33-7.16 (m, 5H), 4.70 (brs, 2H), 4.59 (dd, J = 13.6 Hz, 6.8 Hz, 1H), 4.47 (s, 2H), 1.47 (s, 3H), 1.46 (s, 3H). ^{13}C NMR (100 MHz,

$CDCl_3$) δ 131.5, 129.3, 128.8, 128.0, 127.3, 126.5, 123.9, 47.0, 44.5, 21.8. ESI-MS: m/z calcd for $C_{23}H_{24}F_3N_6$ [M+H] = 441.2 found 441.3.

9-isopropyl-2-(2-(methoxymethyl)pyrrolidin-1-yl)-N-(3-(trifluoromethyl)benzyl)-9H-purin-6-amine (6j). The synthesis of 6j was followed by general procedure to yield 31.49 mg (50.2%) of a compound 6j. ^{1}H NMR (400 MHz, $CDCl_3$) δ 7.73 (s, 1H), 7.72-7.48 (m, 5H), 4.76 (s, 1H), 4.65-4.56 (m, 2H), 3.50-3.44 (m, 1H), 3.25-3.14 (m, 2H), 1.91-1.85 (m, 4H), 1.85-1.76 (m, 2H), 1.50 (d, J = 6.8 Hz, 3H, -CH_3), 1.49 (d, J = 6.8 Hz, 3H, -CH_3). ^{13}C NMR (100 MHz, $CDCl_3$) δ 158.1, 157.8, 142.0, 133.2, 132.2, 132.0, 131.5, 131.4, 129.2, 128.8, 128.7, 123.3, 72.4, 58.2, 47.3, 46.9, 40.4, 28.1, 22.9, 22.5, 21.7, 21.6, 10.9. ESI-MS: m/z calcd for $C_{23}H_{29}F_3N_5O$ [M+H] = 449.2 found 449.3.

N2-(2-aminoethyl)-9-isopropyl-N6-(3-(trifluoromethyl)benzyl)-9H-purine-2,6-diamine (6k). The synthesis of 6k was followed by general procedure to yield 21.9 mg (39.8%) of a compound 6k. ^{1}H NMR (400 MHz, $CDCl_3$) δ 7.86 (s, 1H), 7.72-7.68 (m, 1H), 7.65-7.58 (m, 1H), 7.54 (d, J = 8.0 Hz, 1H), 7.47 (dd, J = 8.0 Hz, 7.6 Hz, 1H), 5.31 (s, 1H), 4.90-4.80 (m, 1H) 4.70-4.62 (m, 1H), 1.54 (s, 3H), 1.53 (s, 3H), 1.43-1.39 (m, 2H), 1.38-1.36 (m, 2H). ^{13}C NMR (100 MHz, $CDCl_3$) δ 153.0, 149.0, 138.0, 133.0, 131.2, 129.3, 125.1, 124.7, 53.7, 40.6, 38.5, 22.2, 17.3. ESI-MS: m/z calcd for $C_{18}H_{23}F_3N_7$ [M+H] = 394.2 found 394.3.

9-isopropyl-2-methoxy-N-(3-(trifluoromethyl)benzyl)-9H-purin-6-amine (6l). The synthesis of 6l was followed by general procedure to yield 18.7 mg (36.6%) of a

compound 6l. ^{1}H NMR (400 MHz, DMSO-d_6) δ 8.47 (s, 1H), 8.08 (s, 1H), 7.73 (s, 1H), 7.71-7.65 (m, 1H), 7.63-7.53 (m, 2H), 4.71 (s, 2H), 4.65-4.60 (m, 1H), 3.79 (s, 3H), 1.50 (s, 3H), 1.49 (s, 3H). ^{13}C NMR (100 MHz, DMSO-d_6) δ 142.0, 139.5, 137.6, 132.0, 131.5, 131.4, 129.3, 128.8, 128.7, 123.8, 123.4, 53.8, 46.3, 42.7, 22.0, 10.9. ESI-MS: m/z calcd for $C_{17}H_{19}F_3N_5O$ [M+H] = 366.2 found 366.2.

2-isopropoxy-9-isopropyl-N-(3-(trifluoromethyl)benzyl)-9H-purin-6-amine (6m). The synthesis of 6m was followed by general procedure to yield 17.9 mg (32.5%) of a compound 6m. ^{1}H NMR (400 MHz, $CDCl_3$) δ 7.74 (s, 1H), 7.66 (s, 1H), 7.59 (d, J = 7.6 Hz, 1H), 7.54 (d, J = 7.6 Hz, 1H), 7.46 (t, J = 7.6 Hz, 1H), 5.25 ppm (dd, J = 12.4 Hz, 6.4 Hz, 1H), 4.90 (brs, 2H), 4.80 (dd, J = 13.2 Hz, 6.8 Hz, 1H), 1.60 (s, 3H), 1.58 (d, J = 6.8 Hz, 6H), 1.37 (d, J = 2.8 Hz, 3H), 1.36 (d, J = 2.8 Hz, 3H). ^{13}C NMR (100 MHz, $CDCl_3$) δ 139.9, 130.9, 129.1, 129.0, 125.0, 124.4, 124.2, 59.9, 51.0, 46.8, 41.0, 23.5, 22.6, 21.9, 11.2. ESI-MS: m/z calcd for $C_{19}H_{23}F_3N_5O$ [M+H] = 394.2 found 394.2.

2-butoxy-9-isopropyl-N-(3-(trifluoromethyl)benzyl)-9H-purin-6-amine (6n). The synthesis of 6n was followed by general procedure to yield 22.4 mg (39.3%) of a compound 6n. ^{1}H NMR (400 MHz, $CDCl_3$) δ 8.21 (brs, 1H), 7.66 (brs, 1H), 7.61-7.58 (m, 1H), 7.56-7.52 (m, 1H), 7.46-7.40 (m, 1H), 4.83 (s, 2H), 4.29 (brs, 2H), 4.15-4.05 (m, 1H), 1.78-1.69 (m, 2H), 1.59 (s, 3H), 1.57 (s, 3H), 1.52-1.40 (m, 2H), 0.99-0.94 (m, 2H), 0.92-0.90 (m, 3H). ESI-MS: m/z calcd for $C_{20}H_{25}F_3N_5O$ [M+H] = 408.2 found 408.3.

The general synthetic procedure of compounds (7). The solution of compound **5** (50 mg, 0.126 mmol) in n-BuOH (6 mL) was treated with DIEA (30.2 μL, 0.19 mmol) and various amines (33.5 mg, 0.38 mmol). The reaction mixture was heated at 120 °C for 48 hr. Solvent was evaporated in vacuo. The residue was purified by prep-HPLC with H_2O-acetonitrile to afford compounds as oil.

9-(1-cyclopropylethyl)-N2-(2-(dimethylamino)ethyl)-N6-(3-(trifluoromethyl)benzyl)-9H-purine-2,6-diamine (7b, NCC007). The synthesis of 7a was followed by general procedure to yield 23.1 mg (41.0%) of a compound 7a. ^{1}H NMR (400 MHz, CD_3OD) δ 8.53 (s, 1H), 8.05 (s, 1H), 7.80 (s, 1H), 7.73 (d, J = 7.6 Hz, 1H), 7.57 (d, J = 7.6 Hz, 1H), 7.49 (dd, J = 8.0 Hz, 7.6 Hz, 1H), 5.70 (s, 2H), 4.89 (dd, J = 13.6 Hz, 6.8 Hz, 1H), 1.63 (s, 3H), 1.62 (m, 5H). ^{13}C NMR (100 MHz, CD_3OD) δ 163.0, 162.8, 162.4, 158.0, 157.5, 134.4, 130.8, 129.3, 125.0, 117.8, 115.7, 114.5, 72.2, 56.6, 43.4, 40.6, 37.0, 20.4, 16.5, 5.0, 4.2. ESI-MS: m/z calcd for $C_{22}H_{29}F_3N_7$ [M+H] = 448.2 found 448.3.

9-(1-cyclopropylethyl)-N2-(2-(dimethylamino)ethyl)-N6-methyl-N6-(3-(trifluoromethyl)benzyl)-9H-purine-2,6-diamine (7c). The synthesis of 7b was followed by general procedure to yield 25.4 mg (45.9%) of a compound 7b. ^{1}H NMR (400 MHz, $CDCl_3$) δ 9.89 (brs, 1H, NH), 7.77 (s, 1H), 7.62-7.47 (m, 4H), 5.69 (s, 1H), 5.15 (s, 1H), 4.12-3.90 (m, 2H), 3.89-3.75 (m, 2H), 3.40-3.25 (m, 3H), 3.18 (s, 1H), 2.91 (s, 3H, -N($C\underline{H}_3$)$_3$), 2.73 (s, 3H, -N($C\underline{H}_3$)$_3$) 1.63 (d, J = 6.8 Hz, 3H, -$C\underline{H}_3$), 1.26 (dd, J = 17.6 Hz, 4.4 Hz, 1H, cyclopropy-H), 0.85-0.75 (m, 1H), 0.62-0.56 (m, 2H), 0.52-0.44 (m, 1H). ^{13}C NMR (125 MHz, $CDCl_3$) δ 163.1, 162.7, 151.8, 131.5, 131.1, 130.9, 129.5,

125.3, 122.6, 117.8, 114.9, 57.3, 55.5, 43.2, 40.9, 37.0, 20.9, 17.1, 4.7, 4.0. ESI-MS: m/z calcd for $C_{23}H_{31}F_3N_7$ [M+H] = 462.3 found 462.3.

N1-(9-(1-cyclopropylethyl)-6-((3-(trifluoromethyl)benzyl)oxy)-9H-purin-2-yl)-N2,N2-dimethylethane-1,2-diamine (7d). The synthesis of 7c was followed by general procedure to yield 31.2 mg (55.3%) of a compound 7c. ^{1}H NMR (400 MHz, $CDCl_3$) δ 7.72 (s, 1H), 7.68 (s, 1H), 7.63 (d, J = 7.60 Hz, 1H), 7.49 (d, J = 8.0 Hz, 1H), 7.42 (dd, J = 7.6 Hz, 1H), 5.51 (s, 2H, Ph-C$\underline{H}_2$-), 3.73-3.71 (m, 1H), 3.64 (t, J = 6.0 Hz, 2H, -HN-C$\underline{H}_2$-), 3.04-2.97 (m, 2H, -HN-CH_2-C$\underline{H}_2$-N$(CH_3)_3$), 2.65 (s, 6H), 1.52 (d, J = 6.8 Hz, 3H), 1.30-1.20 (m, 1H), 0.70-0.62 (m, 1H), 0.50-0.42 (m, 1H), 0.37-0.23 (m, 2H). ^{13}C NMR (100 MHz, $CDCl_3$) δ 160.3, 158.1, 153.8, 137.8, 137.7, 131.3, 129.0, 125.4, 124.8, 124.7, 124.6, 122.7, 115.0, 66.9, 57.5, 56.0, 43.9, 37.7, 20.3, 16.8, 4.5, 4.0. ESI-MS: m/z calcd for $C_{22}H_{28}F_3N_6O$ [M+H] = 449.2 found 449.3.

Cell-based circadian assay. The cell-based circadian assay was carried out as described previously[26]. *Bmal1-dLuc* U2OS cells were cultured in culture medium (DMEM supplemented with 10% fetal bovine serum, 0.29 mg/ml L-glutamine, 100 units/ml penicillin, and 100 mg/ml streptomycin). The cells were suspended and seeded onto 384-well white color solid bottom plates with 20 μL (2,000 cells) per well. After incubation for two days, 50 μL of the explant medium (DMEM supplemented with 2% B27, 10 mM HEPES, 0.38 mg/ml sodium bicarbonate, 0.29 mg/ml L-glutamine, 100 units/ml penicillin, 100 mg/ml streptomycin, 0.1 mg/ml gentamicin, and 1 mM luciferin, pH 7.2) was added to each well, followed by the treatment of 500 nL of compounds (8 μM to 1

nM; 3-fold serial dilution series in DMSO; final 0.7% DMSO). The 384 well plates were sealed with an optically clear film. The luminescence was recorded every 100 min with a microplate reader (Infinite M200, Tecan). The period data was obtained from the luminescence rhythm by curve fitting program CellulaRhythm[20] or MultiCycle (Actimetrics), both of which gave similar results. Due to transient luminescence changes upon the medium change, the first 20-hr data were excluded from the analysis.

***In vitro* kinase assay.** The kinase assays of CKIδ, CKIα, CDK7, and MAPK1 were performed on 384-well plate (10 μL volume) as described previously[26]. The reaction mixture of kinase assays was as follows; for CKIδ, 2 ng/μL CKIδ (Millipore, 14-520), 50 μM peptide substrate RKKKAEpSVASLTSQCSYSS corresponding to human PER2 Lys659-Ser674, and CKI buffer (40 mM Tris, 10 mM $MgCl_2$, 0.5 mM DTT, 0.1 mg/ml BSA, pH 7.5); for CKIα, 1 ng/μl CKIα (Invitrogen, PV3850), 50 μM CKI peptide substrate (Anaspec, 60547-1), and CKI buffer; for CDK7, 5 ng/μl CDK7 (Millipore, 14-476), 100 μM Cdk7/9 peptide substrate (Millipore, 12-526), and CKI buffer; for MAPK1, 1.5 ng/μl ERK2 (Millipore, 14-550), 0.8 μg/μl MBP (Millipore, 13-104), and ERK buffer (50 mM Tris, 10 mM $MgCl_2$, 0.5 mM DTT, 1 mM EGTA, pH7.5). Similarly, 0.75 ng/μl ERK1 (Millipore, 14-439), 0.8 μg/μl MBP (Millipore, 13-104), and ERK buffer were used for MAPK2. 500 nL of compound was added to the reaction mixture (final 5% DMSO). After addition of compounds, the reaction was started by the addition of ATP (final 5 μM). After incubation at 30°C for 3 h, 10 μL of Kinase-Glo Luminescent Kinase Assay reagent (Promega) was added, and luminescence was recorded. The kinase assays of CDK2 were performed by Caliper. IC_{50} values were obtained by using Prism software

(Graph Pad Software). Profiling with longdaysin and NCC007 was done by Caliper and Reaction Biology, respectively.

Molecular Docking. Molecular docking to human CK1α was performed for longdaysin and NCC007. First, the chemical structures of longdaysin and NCC007 were energy-minimized by CHARMm force field, and their 3-D conformers were generated by 'BEST' algorithm (default option with RMSD 1.0 Å) in Discovery Studio software.[31] The conformer generation procedure resulted in 173 and 253 distinct conformations for longdaysin and NCC007, respectively, which were then used to define ligand flexibility during the docking simulation. The input ligand conformers were parametrized by '*molfile_to_params.py'* script to perform molecular docking with RosettaLigand.[32] Overall docking procedure by RosettaLigand was customized by writing xml RosettaScript file to find the lowest binding energy conformation. On the other hand, human CK1α protein structure (PDB code 6GZD) was relaxed with all-heavy-atom constraints to simultaneously minimize Rosetta energy and keep all atoms as close as possible to the original positions in a crystal structure. The center of mass coordinates of native protein-bound ligand (LCI) in 6GZD was used as an initial ligand location in the docking procedure.

Molecular docking was performed by consecutive procedures consisted of low-resolution docking conformation search and all-atom local refinement. In the low resolution docking procedure, the initially-located ligand was 1) randomly translated by 5.0 Å for 50 cycles, 2) rotated by 360 degree for 500 cycles and 3) pulled together by slide movement to ensure the ligand and protein in close proximity. The docking results

were further refined by Rosetta all-atom energy that two rounds of low-repulsive docking/minimization and three rounds of normal docking/minimization procedures were repeatedly performed. All the docking and energy minimization procedures were customized in RosettaScript XML protocol. From 5,000 docking trials, the lowest binding energy conformation in Rosetta Energy Unit (REU) was selected as the most plausible docking model for each ligand (**Figure 4**). We release the atomic coordinates and experimental data upon article publication.

Animals. Adult C57BL/6J background male mice (8 weeks old) were used. They were reared in our animal quarters where environmental conditions were controlled (lights-on, 6:00-18:00; light intensity, approximately 100 lux at the cage bottom; humidity, 60 ± 10%). Mice had free access to food pellets and a water bottle. Experiments were conducted in compliance with the rules and regulations established by the Animal Care and Use Committee of Hokkaido University under with the permission of the Animal Research Committee of Hokkaido University (Approval No. 08-0279).

Circadian behavior measurement. Spontaneous movements were measured using a passive infrared sensor which detects a change in the intensity of thermal radiation from an animal based on movements[29]. The amount of movement was recorded every one min using a computer software (The Chronobiology Kit: Stanford Software System, Santa Cruz, CA, USA). Circadian period of behavioral rhythms was analyzed by regression line obtained from activity onsets. Period differences compare with before administration of compound were expressed as cumulative period.

Surgery. Surgery was performed under isoflurane anesthesia. A handmade guide cannula (inside diameter 0.51 mm, outer diameter 0.81 mm) was stereotaxically inserted into the lateral ventricle (0.2 mm anterior, 1.4 mm lateral, and 2.2 mm from the surface of the skull) and fixed by a dental resin. The osmotic mini-pomp (0.25μl/hr, Model 1002; 0.11μl/hr, Model 1004, Alzet) was connected to the handmade guide cannula via Polyethylene tube (0007750, Alzet). When the osmotic mini-pomp was exchange during recording of behavior, surgery was performed under dim red light.

ASSOCIATED CONTENT

Supporting Information

The Supporting Information is available free of charge on the ACS Publication website.

Table S1. HPLC purity of final compounds.

Figure S1. Docking study of CK1δ.

Figure S2. Comparison of CK1α with CK1δ (NCC007 R-form).

Figure S3. Comparison of CK1α with CK1δ (NCC007 S-form).

Table S2. Profiling of NCC007 toward 374 kinases.

Molecular formula strings of all compounds.

Predicted binding mode of longdaysin to CK1α (PDB)

Predicted binding mode of R-NCC007 to CK1α (PDB)

Predicted binding mode of S-NCC007 to CK1α (PDB)

Predicted binding mode of longdaysin to CK1δ (PDB)

Predicted binding mode of R-NCC007 to CK1δ (PDB)

Predicted binding mode of S-NCC007 to CK1δ (PDB)

Molecular formula strings and associated cell based assay data (CSV)

Accession Codes

PDB code 6GZD and 4HGT were used for docking study of CKIα and CKIδ with compounds, respectively.

AUTHOR INFORMATION

Corresponding Authors

*J.W.L.: phone, +82(0)2 336503514; email, jwlee5@kist.re.kr

*T.H.: phone, +81(0)52 747 6356; email, thirota@itbm.nagoya-u.ac.jp

ORCID

Tsuyoshi Hirota: 0000-0003-4876-3608

ACKNOWLEDGMENTS

This work was partially supported by National Research Council of Science & Technology (NST) grant by the Korea government (MSIP) (No. CRC-15-04-KIST) for JWL, the Kanae Foundation for the Promotion of Medical Science and the Kowa Life Science Foundation for TH, and the Ministry of Oceans and Fisheries, Korea (Grant No. 20170449) for KP.

ABBREVIATIONS USED

CKI, casein kinase I; CLOCK, Circadian Locomotor Output Cycles Kaput; BMAL1, Brain and Muscle Aryl hydrocarbon receptor nuclear translocator-Like; Per, Period; Cry,

Cryptochrome; SCN, suprachiasmatic nucleus; FASP, familiar advanced sleep phase; MAPK, mitogen-activated protein kinase; CDK, cyclin dependent kinase; SAR, structure activity relationship; SRPK, Serine/arginine-rich protein specific kinase; CLK, Cdc2-like kinase; ANOVA, analysis of variance

REFERENCES

(1) Takahashi, J. S.; Hong, H. K.; Ko, C. H.; McDearmon, E. L. The genetics of mammalian circadian order and disorder: implications for physiology and disease. *Nat. Rev. Genet.* **2008**, *9*, 764-775.

(2) Reppert, S.M.; Weaver, D.R. Coordination of circadian timing in mammals. *Nature* **2002**, *418*, 935-941.

(3) Schibler, U.; Sassone-Corsi, P. A. Web of circadian pacemakers. *Cell* **2002**, *111*, 919-922.

(4) Storch, K. –F.; Paz, C.; Signorovitch, J.; Raviola, E.; Pawlyk, B.; Li, T.; Weitz, C. J. Intrinsic circadian clock of the mammalian retina: importance for retinal processing of visual information. *Cell* **2007**, *130*, 730-741.

(5) Zhang, E. E.; Liu, Y.; Dentin, R.; Pongsawakul, P. Y.; Liu, A. C.; Hirota, T.; Nusinow, D. A.; Sun, X.; Landais, S.; Kodama, Y.; Brenner, D. A.; Montminy, M.; Kay, S. A. Cryptochrome mediates circadian regulation of cAMP signaling and hepatic gluconeogenesis. *Nat. Med.* **2010**, *16*, 1152-1156.

(6) Sheward, W. J.; Naylor, E.; Knowles-Barley, S.; Armstrong, J. D.; Brooker, G. A.; Seckl, J. R.; Turek, F. W.; Holmes, M. C.; Zee, P. C.; Harmar, A. J. Circadian control

of mouse heart rate and blood pressure by the suprachiasmatic nuclei: behavioral effects are more significant than direct outputs. *PLoS One.* **2010**, *22*, e9783.

(7) Bass, J.; Mitchell, A. L. Circadian time signatures of fitness and disease. *Science* **2016**, *354*, 994-999

(8) Musiek, E. S.; Holtzman, D. M. Mechanisms linking circadian clocks, sleep, and neurodegeneration. *Science* **2016**, *354*, 1004-1008.

(9) Takeda, N.; Maemura, K. Circadian clock and cardiovascular disease. *J. Cardiol.* **2011**, *57*, 249-256.

(10) Sahar, S.; Sassone-Corsi, P. Metabolism and cancer: the circadian clock connection. *Nat. Rev. Cancer* **2009**, *12*, 886-896

(11) Panda S. Circadian physiology of metabolism. *Science* **2016**, *354*, 1008-1015.

(12) Hirano, A.; Fu, Y. H.; Ptáček, L. J. The intricate dance of post-translational modifications in the rhythm of life. *Nat. Struct. Mol. Biol.* **2016**, *23*, 1053-1060.

(13) Eckel-Mahan, K.; Sassone-Corsi, P. Metabolism control by the circadian clock and vice versa. *Nat. Struct. Mol. Biol.* **2009**, *16*, 462-467.

(14) Robles, M. S.; Humphrey, S. J.; Mann, M. Phosphorylation is a central mechanism for circadian control of metabolism and physiology. *Cell Metab.* **2017**, *25*, 118-127.

(15) Eide, E. J.; Woolf, M. F.; Kang, H.; Woolf, P.; Hurst, W.; Camacho, F.; Vielhaber, E. L.; Giovanni, A.; Virshup, D. M. Control of mammalian circadian rhythm by CKIε-regulated proteasome-mediated PER2 degradation. *Mol. Cell. Biol* **2005**, 25, 2795-2807.

(16) Xu, Y.; Padiath, Q. S.; Shapiro, R. E.; Jones, C. R.; Wu, S. C.; Saigoh, N.; Saigoh, K.; Ptácek, L. J.; Fu, Y. H. Functional consequences of a CKIdelta mutation causing familial advanced sleep phase syndrome. *Nature* **2005**, *434*, 640-644.

(17) Toh, K. L.; Jones, C. R.; He, Y.; Eide, E. J.; Hinz, W. A.; Virshup, D. M.; Ptácek, L. J.; Fu, Y. H. An hPer2 phosphorylation site mutation in familial advanced sleep phase syndrome. *Science* **2001**, *291*, 1040-1043.

(18) Liu, A. C.; Lewis, W. G.; Kay, S. A. Mammalian circadian signaling networks and therapeutic targets. *Nat. Chem. Biol.* **2007**, *3*, 630-639.

(19) Chen, Z.; Yoo, S. H.; Takahashi, J. S. Development and therapeutic potential of small-molecule modulators of circadian systems. *Annu. Rev. Pharmacol. Toxicol.* **2018**, *58*, 231-252.

(20) Hirota, T.; Lewis, W. G.; Liu, A. C.; Lee, J. W.; Schultz, P. G.; Kay, S. A. A chemical biology approach reveals period shortening of the mammalian circadian clock by specific inhibition of GSK-3β. *Proc. Natl. Acad. Sci. USA* **2008**, *105*, 20746-20751.

(21) Hayashi, Y.; Sanada, K.; Hirota, T.; Shimizu, F.; Fukada, Y. p38 Mitogen-activated protein kinase regulates oscillation of chick pineal circadian clock. *J. Biol. Chem.* **2003**, *28*, 25166–25171.

(22) Chansard, M.; Molyneux, P.; Nomura, K.; Harrington, M. E.; Fukuhara,C. c-Jun N-therminal kinase inhibitor SP600125 modulates the period of mammalian circadian rhythms. *Neuroscience* **2007**, *145*, 812–823.

(23) Badura, L.; Swanson, T.; Adamowicz, W.; Adams, J.; Cianfrogna, J.; Fisher, K.; Holland, J.; Kleiman, R.; Nelson, F.; Reynolds, L.; Germain, K. S.; Schaeffer, E.;

Tate, B.; Sprouse, J. An inhibitor of casein kinase Iε induces phase delays in circadian rhythms under free-running and entrained. *J. Pharmacol. Exp. Ther.* **2007**, *322*, 730-738.

(24) Vanselow, K.; Vanselow, J. T.; Westermark, P. O.; Reischl, S.; Maier, B.; Korte, T.; Herrmann, A.; Herzel, H.; Schlosser, A.; Kramer, A. Differential effects of PER2 phosphorylation: molecular basis for the human familial advanced sleep phase syndrome (FASPS). *Genes Dev*., **2006**, *20*, 2660–2672.

(25) Reischl, S.; Vanselow, K.; Westermark, P. O.; Thierfelder, N.; Maier, B.; Herzel, H.; Kramer, A. β-TrCP1-mediated degradation of PERIOD2 is essential for circadian dynamics. *J. Biol. Rhythms* **2007**, *22*, 375-386.

(26) Hirota, T.; Lee, J. W.; Lewis, W. G.; Zhang, E. E.; Breton, G.; Liu, X.; Garcia, M.; Peters, E. C.; Etchegaray, J. –P.; Traver, D.; Schultz, P. G.; Kay, S. A. High-throughput chemical screen identifies a novel potent modulator of cellular circadian rhythms and reveals CKIα as a clock regulatory kinase. *PLoS Biol.* **2010**, *8*, e1000559.

(27) The PyMOL Molecular Graphics System, Version 1.2r3pre, Schrödinger, LLC.

(28) Laskowski, R. A.; Swindells, M. B., LigPlot+: multiple ligand-protein interaction diagrams for drug discovery. *J. Chem. Inf. Model.*, **2011**, *51*, 2778-2786.

(29) Abe, H.; Honma, S.; Ohtsu, H.; Honma, K., Circadian rhythms in behavior and clock gene expressions in the brain of mice lacking histidine decarboxylase. *Mol. Brain Res.* **2004**, *124*, 178-187.

(30) Meng, Q. J.; Maywood, E. S.; Bechtold, D. A.; Lu, W. Q.; Li, J.; Gibbs, J. E.; Dupré, S. M.; Chesham, J. E.; Rajamohan, F.; Knafels, J.; Sneed, B.; Zawadzke, L. E.; Ohren, J. F.; Walton, K. M.; Wager, T. T.; Hastings, M. H.; Loudon, A. S., Entrainment of

disrupted circadian behavior through inhibition of casein kinase 1 (CK1) enzymes. *Proc Natl Acad Sci U S A*. **2010**, *107*, 15240-15245.

(31) Discovery Studio **2018** (San Diego: Dassault Systèmes)

(32) Lemmon, G.; Meiler, J., Rosetta ligand docking with flexible XML protocols. *Methods Mol Biol* **2012**, *819*, 143-155.

Table of Contents graphic

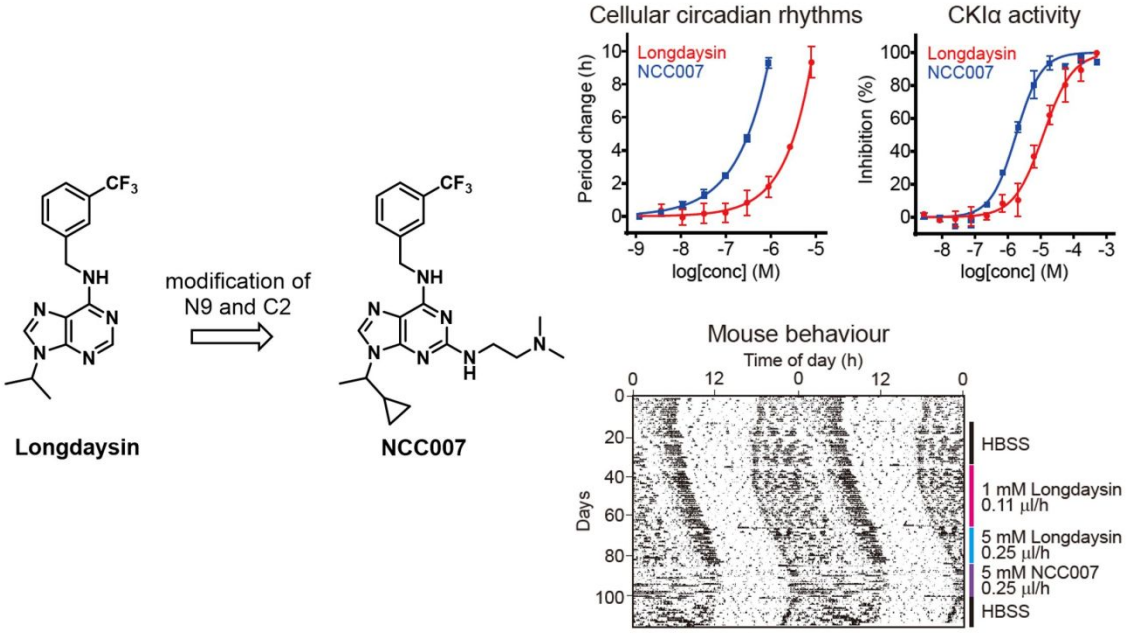

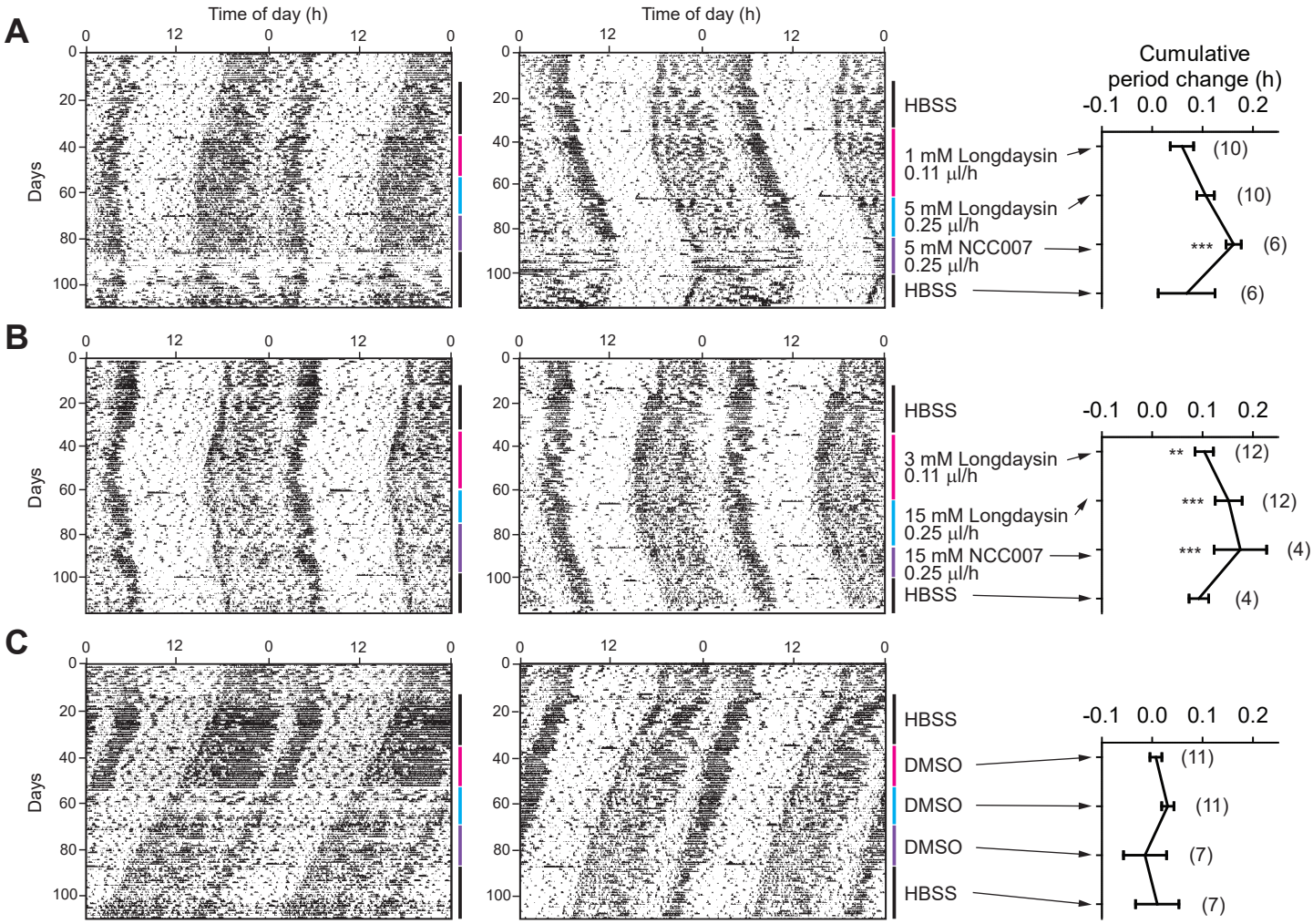
A
B
C
Time of day (h)
Days
HBSS
1 mM Longdaysin
0.11 µl/h
5 mM Longdaysin
0.25 µl/h
5 mM NCC007
0.25 µl/h
3 mM Longdaysin
0.11 µl/h
15 mM Longdaysin
0.25 µl/h
15 mM NCC007
0.25 µl/h
DMSO
Cumulative
period change (h)
-0.1 0.0 0.1 0.2
(10)
(6)
(12)
(4)
(11)
(7)
**
***

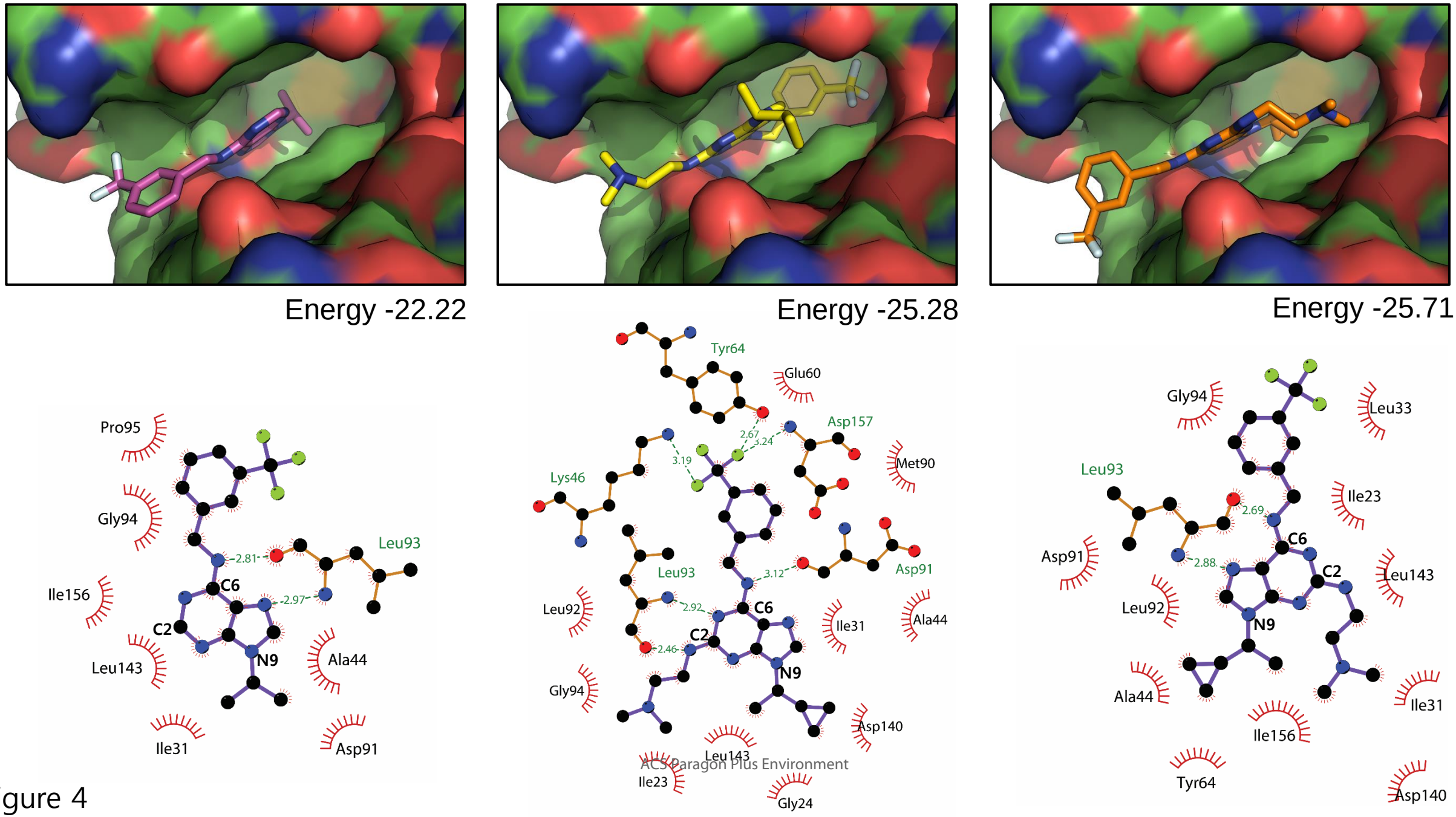

Figure 4

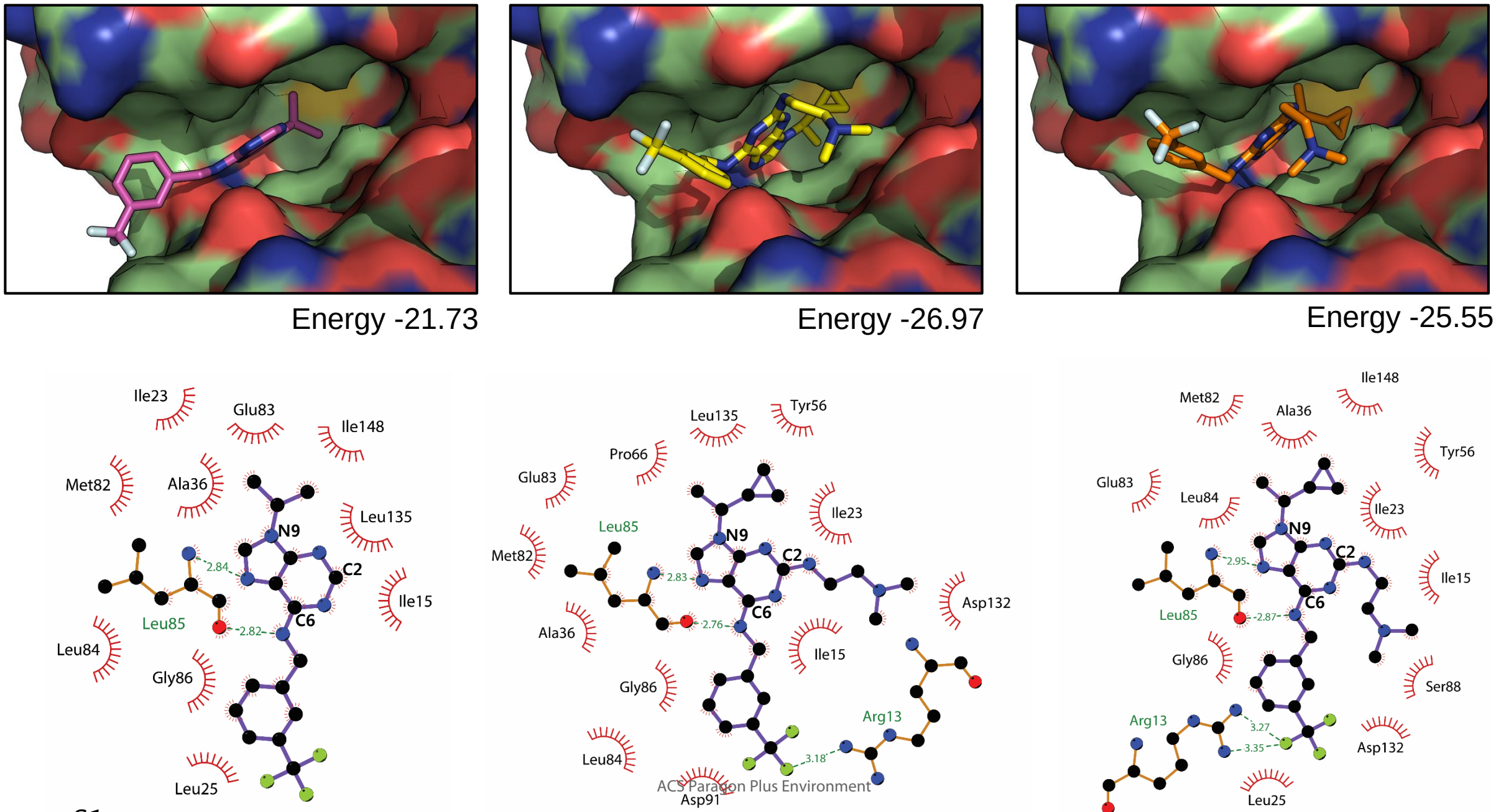
A
B
C
Energy -21.73
Energy -26.97
Energy -25.55
Ile23
Glu83
Ile148
Met82
Ala36
Leu135
N9
C2
Ile15
Leu85
C6
Leu84
Gly86
Leu25
2.84
2.82
Tyr56
Pro66
2.83
2.76
Asp132
Arg13
3.18
Asp91
Ser88
3.27
3.35
ACS Paragon Plus Environment

Figure S1

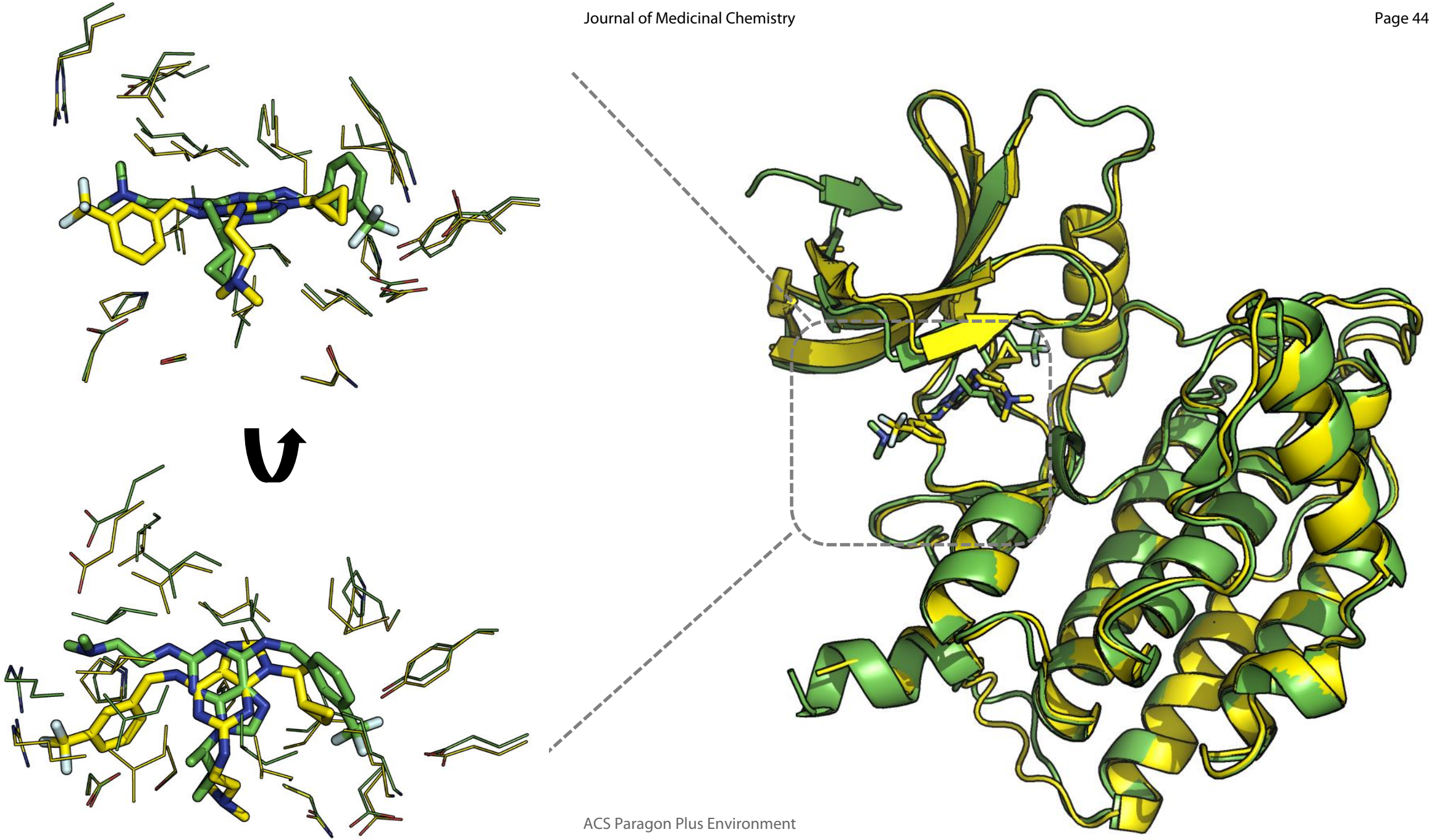

Figure S2

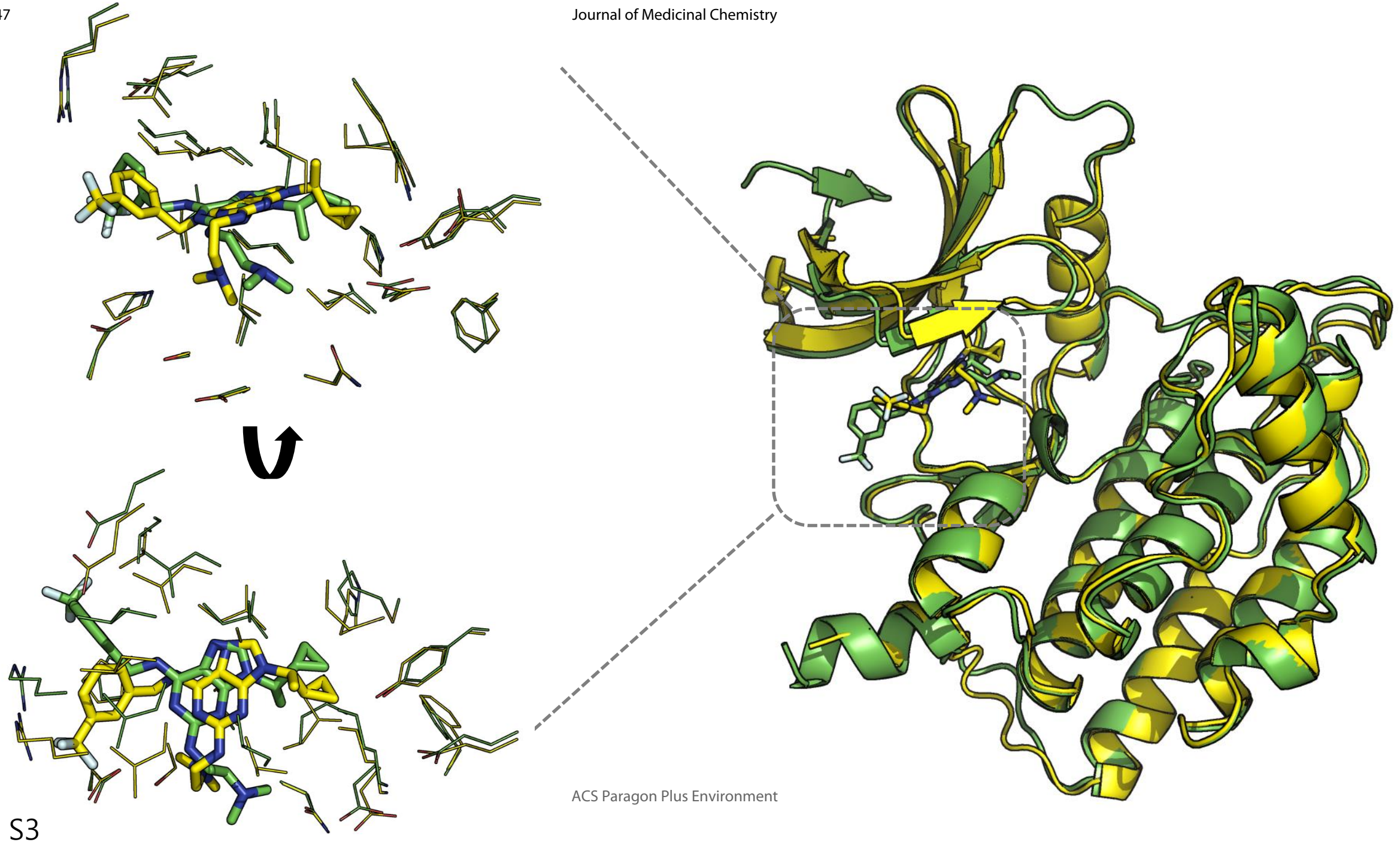

Figure S3

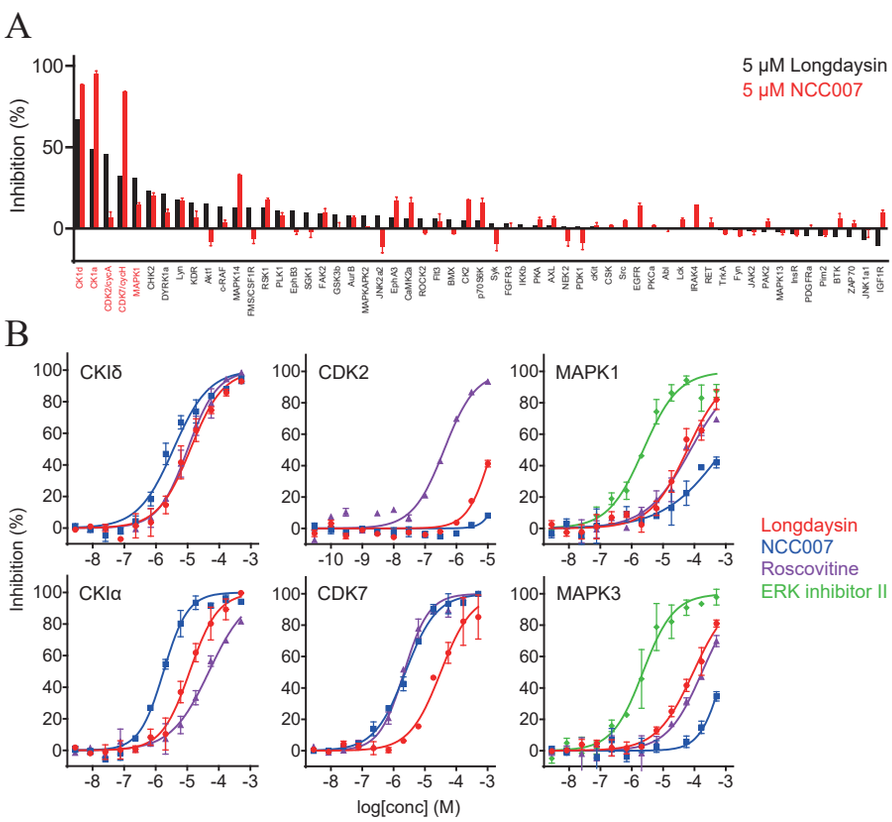

	IC_{50} (μM)					
	CKIδ	CKIα	CDK2	CDK7	MAPK1	MAPK3
Longdaysin	12	12	13	32	59	92
NCC007	3.6	1.8	37	2.4	850	830
Roscovitine	10	49	0.4	2.2	75	170

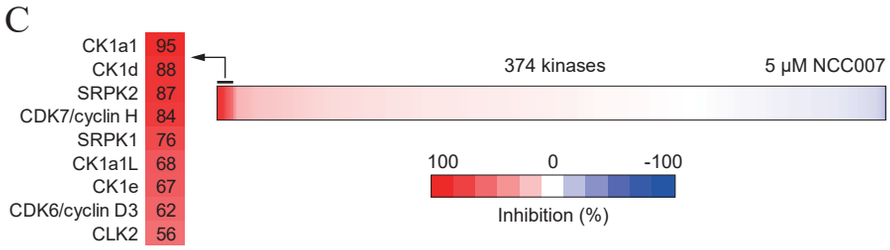

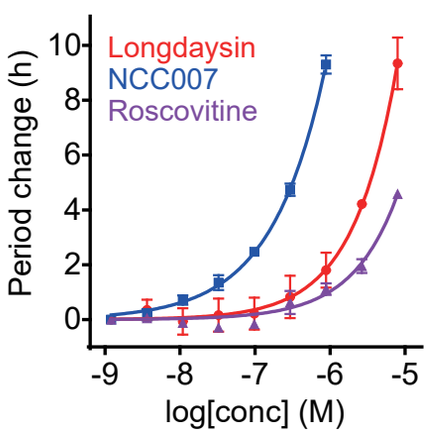

	1 hr (μM)	5 hr (μM)
Longdaysin	0.39	3.4
NCC007	0.022	0.32
Roscovitine	0.96	9.0